Faraday Discussions

Single-crystalline oligomer-based conductors modeling the doped poly(3,4-ethylenedioxythiophene) family

Journal:	*Faraday Discussions*
Manuscript ID	FD-ART-07-2023-000134.R1
Article Type:	Paper
Date Submitted by the Author:	20-Jul-2023

Complete List of Authors:	Fujino, Tomoko; The University of Tokyo, The Institute for Solid State Physics Kameyama, Ryohei; The University of Tokyo, The Institute for Solid State Physics Onozuka, Kota; The University of Tokyo, The Institute for Solid State Physics Matsuo, Kazuki; The University of Tokyo, The Institute for Solid State Physics Dekura, Shun; The University of Tokyo, The Institute for Solid State Physics Yoshimi, Kazuyoshi; The University of Tokyo, The Institute for Solid State Physics Mori, Hatsumi; The University of Tokyo, The Institute for Solid State Physics

PAPER

Single-crystalline oligomer-based conductors modeling the doped poly(3,4-ethylenedioxythiophene) family

Received 00th January 20xx,
Accepted 00th January 20xx

DOI: 10.1039/x0xx00000x

Tomoko Fujino*, Ryohei Kameyama, Kota Onozuka, Kazuki Matsuo, Shun Dekura, Kazuyoshi Yoshimi, Hatsumi Mori*

Conductive polymers with highly conjugated systems, such as the doped poly(3,4-ethylenedioxythiophene) (PEDOT) family, are commonly used in organic electronics. However, their structural inhomogeneity with various chain lengths makes it difficult to control their conductivities and structural details. On the other hand, low-molecular-weight materials have well-defined structures but relatively narrow conjugate areas with a limited range of Coulomb repulsion between carriers (U_{eff}), which hamper the flexible control of conductivities. To bridge this gap, we developed oligomer-based conductors, which are intermediate materials between polymers and low-molecular-weight materials. Using a library of single-crystal charge-transfer salts of oligo(3,4-ethylenedioxythiophene) (oligoEDOT) analogs that model the doped PEDOT family, we have investigated the structure-determining factors affecting their conductivities, such as counter anion variations, lengths of oligomer donor, and band fillings. Through the screening study, we developed oligoEDOT analogs with tunable room temperature conductivities by several orders of magnitude, including a metallic state above room temperature. In this study, we consistently evaluated the electronic structural insights by first-principles calculations and revealed that U_{eff} is the dominant factor that determines the relationship between the structures and conductivities. The unique feature of oligoEDOT conductor systems with widely variable U_{eff} can differentiate these systems from strongly electron-correlated systems.

Introduction

Organic conductor materials are lightweight, flexible, solution-processible in a cost-effective and energy-saving manner, and rich in structural designability.[1] The use of organic conductors has advanced the application of organic electronic devices in the Internet of Things

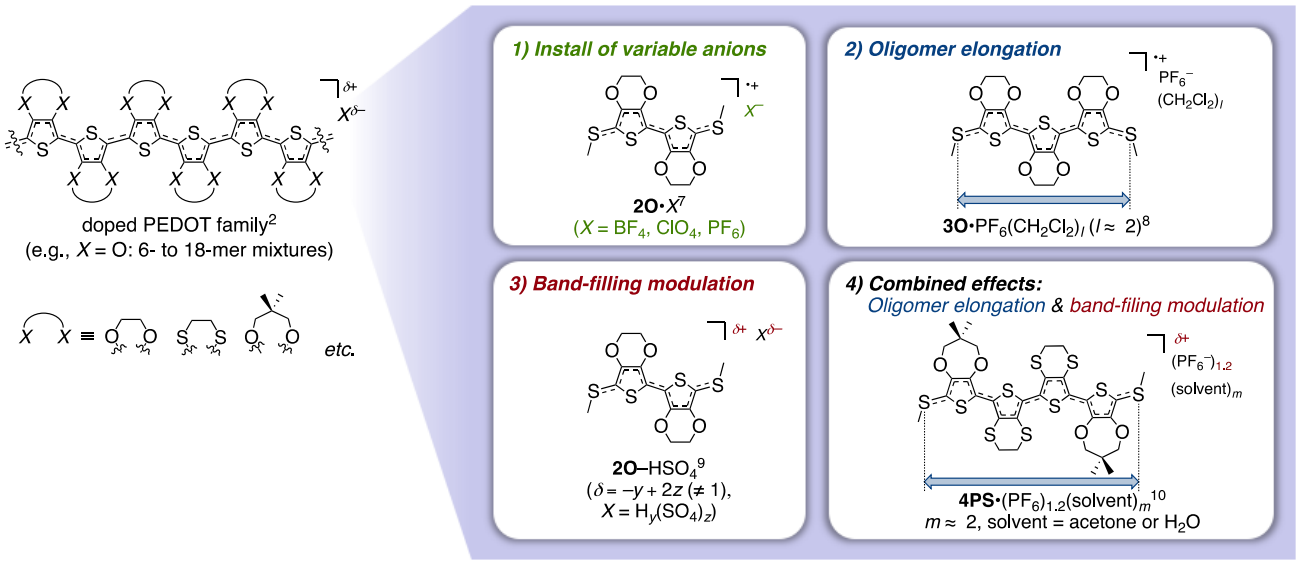

Figure 1. Chemical structures of doped PEDOT, **2O•***X*, **3O•**$PF_6(CH_2Cl_2)_I$, **2O**–HSO_4, and **4PS•**$(PF_6)_{1.2}(solvent)_m$.

[a] The Institute for Solid State Physics, The University of Tokyo, 5-1-5 Kashiwanoha, Kashiwa, Chiba 277-8581, Japan

technologies. Notably, the precise and flexible control of conductivity, as well as high reproducibility, must be realized toward the development of organic conductors applicable in next-generation organic electronics. Conductive polymers with highly π-conjugated systems, such as the doped poly(3,4-ethylenedioxythiophene) (PEDOT) family (Figure 1),[2] are widely used in organic electronics. However, these polymers exhibit various chain lengths, and their structural inhomogeneities often result in limited precise control over their conductivities. The poor accessibility of their structural details also hinders the understanding of the mechanism underlying conductivity control. In contrast, low-molecular-weight materials can be characterized by single-crystal X-ray diffraction (XRD). The structure–conductivity relationships address the conduction mechanisms,[3] in which conductivity is basically defined by the ratio of the Coulomb repulsion between carriers ($\boldsymbol{U}_{\mathrm{eff}}$) and intermolecular interaction ($\boldsymbol{W}$), i.e., $\boldsymbol{U}_{\mathrm{eff}}/\boldsymbol{W}$.[4] However, the relatively narrow conjugate areas have often limited the range of $\boldsymbol{U}_{\mathrm{eff}}$, hampering the flexible control of their conductivities.

Recently researchers have focused on an intermediate between conductive polymers and low-molecular-weight conductors, i.e., oligomer-based conductors.[5] Single-crystalline oligomer conductors have well-characterized structures at the atomic level and various structure-determining factors such as oligomer length and sequence. Especially, the expandable π-conjugated systems possibly exhibit a wide range of $\boldsymbol{U}_{\mathrm{eff}}$. Also, these factors can spatially adjust the packing structures (i.e., $\boldsymbol{W}$), enabling control conductivity in a precise and flexible manner dually by $\boldsymbol{U}_{\mathrm{eff}}$ and $\boldsymbol{W}$. Among oligomers, oligo(3,4-ethylenedioxythiophene) (oligoEDOT) analogs that model the PEDOT family[2] have great potential as organic conductor materials for the future. However, the synthesis to expand these highly π-conjugated systems in the doped states (i.e., radical cationic salts) has been challenging, and no successful examples were reported except for that without π-stacking.[6] We have synthesized a library of single-crystal oligoEDOT analogs in doped forms and investigated their conductivities.[7–10] We identified the factors that influence the conductivities, such as 1) install of variable counter anions, 2) oligomer elongation, 3) band-filling modulations, and 4) their combined effects (Figure 1). Through the screening study, we developed charge-transfer systems that showed room temperature conductivities varied by several orders of magnitude, including highly conducting material in a metallic state above room temperature. In this study, we consistently evaluated the electronic structural insights by first-principles calculations based on the single-crystal structures, addressing the structure–physical property relationship that was dominated by $\boldsymbol{U}_{\mathrm{eff}}$. We discovered the electronic features unique to oligoEDOT-based conductors with widely tunable $\boldsymbol{U}_{\mathrm{eff}}$, which can differentiate these systems from strongly electron-correlated systems.

Results and discussion

Shortest oligomer conductor used to model doped PEDOT

We synthesized a single crystal of a charge-transfer salt of the shortest oligomer **2O**.[7] First, we dimerized monomer unit **O** (3,4-ethylenedioxythiophene) via a Cu-mediated homocoupling reaction. Electrooxidation of **2O** with $^{n}Bu_4N{\bullet}PF_6$ ($^{n}Bu_4N$ = tetra-*n*-butylammonium) as the electrolyte at an electrical current of 0.3 μA yielded single-crystal **2O**•PF_6. Single-crystal XRD results revealed a 1:1 donor-to-anion molar ratio (Figure 2a,b), indicating a half-filled electronic state. The space group is categorized as $P2_1/n$, with molecule-independent donors (Table 1). The donors are stacked in a column-like structure in a head-to-tail manner, with the anions forming short contacts between the S atoms of the donors and the F atoms of the anions (d_{SF} = 3.056(3) Å; Figure 2a), which is shorter than the sum of van der Waals radii of the S and F atoms (3.27 Å). The donors are equivalently π-stacked with a π–π stacking distance of 3.481 Å (Figure 2b). The donor's Wannier function (corresponding to the molecular orbitals of the donor in a radical cation form) extends throughout the molecule to the S atoms at both termini (Figure 2c), as confirmed by first-principles calculations (combined Quantum ESPRESSO (QE)[11,12] and RESPACK[14]

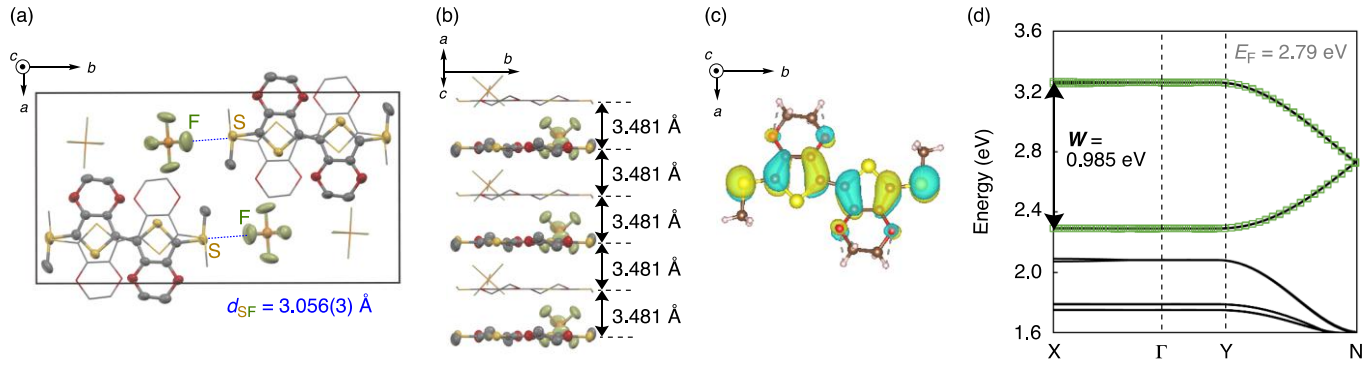

Figure 2. Structures of single-crystal **2O**•PF_6 in the major-occupancy at 293 K. (a, b) Single-crystal structure along (a) the *a*-axis (a) and (b) perpendicular to the π-stacking direction.[6] (c) QE[11,12]/RESPACK[14]-calculated maximally localized Wannier functions viewed along the *c*-axis, as visualized using VESTA.[13] (d) QE[11,12]-calculated band structure. X (0.5,0,0), Γ (0,0,0), Y (0,0.5,0), N (0,0.5,0.5). Atoms were colored as follows; red: oxygen; yellow: sulfur; gray: carbon; yellowish green: fluorine; orange: phosphorous, white: hydrogen. Hydrogens were omitted for clarity (a,b).

packages) based on the single-crystal structure. The density of states was calculated using QE to determine the band structure and $\boldsymbol{W}$ to be 0.985 eV (Figure 2d). These data indicate the strong intracolumnar orbital interactions between the donors, whose $\boldsymbol{W}$ value is consistent

with those of typical metals and superconductors.[3] This large ***W*** may be characteristic of oligoEDOT systems with molecular orbitals spread over the entire donor molecules containing multiple relatively large S atoms and overlayed tightly in a head-to-tail fashion with a relatively short π–π stacking distance. Notably, the bands at the Fermi level did not display a gap, thus exhibiting a metallic electronic state unless $\boldsymbol{U}_{\mathbf{eff}}$ is considered.

In contrast, the temperature dependence of the electrical resistivity (ρ) of **2O**•PF_6 induces the semiconducting behavior, with an activation energy (E_a) of 0.278 eV around room temperature, according to the Arrhenius plot.[7] The electrical resistivity at room temperature (ρ_{rt}) is 4.3 × 10^4 Ω cm,[7] which is modest for semiconductors and several orders of magnitude higher than that of doped PEDOT.[2] Considering the band structure suggests a metallic electronic state, wherein the contribution of $\boldsymbol{U}_{\mathbf{eff}}$ is ignored, this discrepancy suggests the presence of a large $\boldsymbol{U}_{\mathbf{eff}}$ above ***W*** (i.e., $\boldsymbol{U}_{\mathbf{eff}} > \boldsymbol{W}$), reminiscent of a rare half-filled Mott insulator state. Equation $2E_a = \boldsymbol{U}_{\mathbf{eff}} - \boldsymbol{W}$, used for strongly correlated systems, estimated the experimental $\boldsymbol{U}_{\mathbf{eff}}$ ($\boldsymbol{U}_{\mathbf{eff}}^{\mathbf{exp}}$) to be 1.53.[8] The ratio $\boldsymbol{U}_{\mathbf{eff}}/\boldsymbol{W}$, as an indicator of conductivity (i.e., $\boldsymbol{U}_{\mathbf{eff}}/\boldsymbol{W} \leq 1$: metals; $\boldsymbol{U}_{\mathbf{eff}}/\boldsymbol{W} > 1$: semiconductors or insulators),[4] suggests that strategies to increase ***W*** or decrease $\boldsymbol{U}_{\mathbf{eff}}$ may improve the conductivity.

Effect of installed anions in charge-transfer salt (2O•*X*)

Reducing the π–π stacking distance by introducing small counter anions generally increases the ***W***. This may also increase the intermolecular Coulomb repulsion, resulting in shielding effects of electrons to reduce $\boldsymbol{U}_{\mathbf{eff}}$. Thus, we installed ClO_4^- and BF_4^- as the counter anions for **2O** charge-transfer salts.[7] The anions were smaller than the PF_6^- anion, with sizes of 5.1 Å (PF_6^-) > 4.9 Å (ClO_4^-) > 4.8 Å (BF_4^-) (Table 1). The packing structures were both categorized as *I*2/*a* with half-molecule-independent donors (Figure 3a, Table 1). The donor-to-anion molar ratios in **2O**•BF_4 and **2O**•ClO_4 were both 1:1, indicating that the donor's valency is +1, as observed in **2O**•PF_6. The ethylene groups of the donors in **2O**•BF_4 and **2O**•ClO_4 are disordered in a 1:1 ratio. Unlike in **2O**•PF_6, no short contacts were observed between the donors and anions. The order of the π–π stacking distance depends strongly on the anion size: 3.481 Å (**2O**•PF_6) > 3.471 Å (**2O**•ClO_4) > 3.462 Å (**2O**•BF_4). We evaluated the ***W*** values of **2O**•ClO_4 and **2O**•BF_4 for the first time by QE[11,12] to be 0.979 and 1.01 eV (Table 1), respectively. Consistently large ***W*** values (≈ 1.0 eV) may be characteristic of the electronic structures of oligoEDOT conductors. The ***W*** values for **2O**•ClO_4 and **2O**•BF_4 were higher than or comparable to **2O**•PF_6. Notably, the greater π–π stacking distance (**2O**•PF_6 > **2O**•ClO_4 > **2O**•BF_4) did not reduce the corresponding ***W*** values in the order predicted **2O**•PF_6 < **2O**•ClO_4 < **2O**•BF_4; experimental **2O**•ClO_4 < **2O**•PF_6 < **2O**•BF_4), indicating the dominant contribution of the hidden $\boldsymbol{U}_{\mathbf{eff}}$ in the calculations.

Table 1. Structural data and electronic parameters of **2O**•*X* (*X* = PF_6, ClO_4, and BF_4) single crystals.

Compound	**2O**•PF_6	**2O**•ClO_4	**2O**•BF_4
Experimental			
Space group, *Z*	$P2_1/n$, 4[7]	$I2/a$, 4[7]	$I2/a$, 4[7]
Donor-stacking form	head-to-tail[7]	head-to-tail[7]	head-to-tail[7]
Donor valence δ	1[7]	1[7]	1[7]
π–π stacking distance[a] (Å)	3.481[7]	3.471[7]	3.462[7]
ρ_{rt} (Ω cm)	4.3 × 10^4 [7]	4.3 × 10^3 [7]	2.8 × 10^2 [7]
E_a (eV; the value around room temperature)	0.278[7]	0.224[7]	0.177[7]
$\boldsymbol{U}_{\mathbf{eff}}^{\mathbf{exp}}$ [b]	1.54[8]	1.43	1.36
$\boldsymbol{U}_{\mathbf{eff}}^{\mathbf{exp}}$ [b]/***W***	1.56[8]	1.46	1.35
Theoretical			
W (eV) [QE[11,12]/RESPACK[14]]	0.985[10]	0.979	1.01
$\boldsymbol{U}_{\mathbf{eff}}^{\mathbf{calc}}$ (eV) [QE[11,12]/RESPACK[14]]	2.43[10]	2.33	2.35
$\boldsymbol{U}_{\mathbf{eff}}^{\mathbf{calc}}/\boldsymbol{W}$	2.46	2.38	2.34

[a]Interplanar π–π stacking distances were measured between the mean planes comprising 10 atoms in the thiophene rings of **2O**. [b]$\boldsymbol{U}_{\mathbf{eff}}^{\mathbf{exp}} = \boldsymbol{W} + 2E_a$.

On the other hand, the ρ_{rt} values are 4.3 × 10^3 Ω cm for **2O**•ClO_4 and 2.8 × 10^2 Ω cm for **2O**•BF_4 (Figure 3b, Table 1), which are one to two orders of magnitude lower than that of **2O**•PF_6 (4.3 × 10^4 Ω cm). The temperature dependencies showed the semiconducting behavior, with lower E_a values of 0.224 eV (**2O**•ClO_4) and 0.177 eV (**2O**•BF_4) (Figure 3b, Table 1). Generally, the larger the ***W***, the smaller the E_a. However, the E_a order (**2O**•PF_6 > **2O**•ClO_4 < **2O**•BF_4) was inconsistent with that predicted (i.e., **2O**•ClO_4 > **2O**•PF_6 > **2O**•BF_4) from the experimental ***W*** order (**2O**•ClO_4 < **2O**•PF_6 < **2O**•BF_4). This discrepancy is also reminiscent of the dominant contribution of $\boldsymbol{U}_{\mathbf{eff}}$ in their conductivity.

Therefore, we quantified $\boldsymbol{U}_{\mathbf{eff}}$ from the experimental results and through first-principles calculations for the first time. ~~W~~We first determined the $\boldsymbol{U}_{\mathbf{eff}}$ values experimentally using the E_a and calculated ***W*** values under the extended Hubbard model (i.e., $\boldsymbol{U}_{\mathbf{eff}}^{\mathbf{exp}} = \boldsymbol{W} + 2E_a$). The $\boldsymbol{U}_{\mathbf{eff}}^{\mathbf{exp}}$ values were determined to be 1.54 eV for **2O**•PF_6, 1.43 eV for **2O**•ClO_4, and 1.36 eV for **2O**•BF_4; whereas the $\boldsymbol{U}_{\mathbf{eff}}^{\mathbf{exp}}/\boldsymbol{W}$ were determined to be 1.56 for **2O**•PF_6, 1.46 for **2O**•ClO_4, and 1.35 for **2O**•BF_4. The order of the $\boldsymbol{U}_{\mathbf{eff}}^{\mathbf{exp}}/\boldsymbol{W}$ values is comparable to that of E_a and

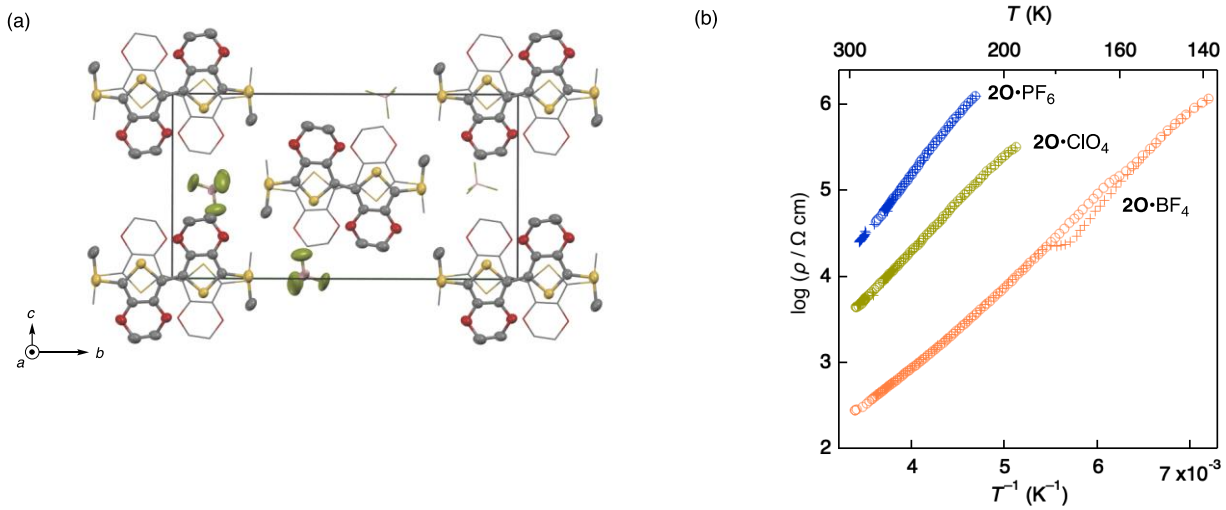

Figure 3. (a) Single-crystal structure of **2O**•BF_4 along the *c*-axis.[7] Atoms were colored as follows; red: oxygen; yellow: sulfur; gray: carbon; yellowish green: fluorine; pink: boron. Hydrogens were omitted for clarity. (b) Electrical conductivities of **2O**•*X* (*X* = PF_6, ClO_4, and BF_4).[7] Cooling (open circles) and heating (plus marks) processes are shown.

ρ_{rt} (**2O**•PF_6 > **2O**•ClO_4 > **2O**•BF_4). We then investigated the dominant parameter $\boldsymbol{U}_{\mathbf{eff}}$ with theoretical calculations to address the intrinsic values based on the single-crystal structures using QE[11,12] and RESPACK[14] packages (i.e., $\boldsymbol{U}_{\mathbf{eff}}^{\mathbf{calc}}$) for the first time in oligoEDOT conductor systems. The $\boldsymbol{U}_{\mathbf{eff}}^{\mathbf{calc}}$ values are listed in order, as follows: 2.43 eV (**2O**•PF_6) > 2.33 eV (**2O**•ClO_4) ≈ 2.35 eV (**2O**•BF_4) (Table 1). Favorably reduced $\boldsymbol{U}_{\mathbf{eff}}$ values were observed for **2O**•BF_4 and **2O**•ClO_4 owing to their shorter π–π stacking distances, which may provide relatively large shielding effects for $\boldsymbol{U}_{\mathbf{eff}}$. The resulting $\boldsymbol{U}_{\mathbf{eff}}^{\mathbf{calc}}/\boldsymbol{W}$ values are 2.46 (**2O**•PF_6) > 2.38 (**2O**•ClO_4) > 2.34 (**2O**•BF_4) (Table 1); this order is consistent with the orders of ρ_{rt} and E_a. Therefore, it can be deduced that both $\boldsymbol{U}_{\mathrm{eff}}$ and $\boldsymbol{W}$ were affected by the variations of installed counter anions, cooperatively reducing $\boldsymbol{U}_{\mathbf{eff}}/\boldsymbol{W}$ by balancing the $\boldsymbol{W}$ and $\boldsymbol{U}_{\mathbf{eff}}$ and thus improving the electrical conductivity. It is noted that the $\boldsymbol{U}_{\mathbf{eff}}^{\mathbf{calc}}$ values of salts with high conductivities can be overestimated because their shielding effects are less effective for highly conducting materials. Future calculations involving the contribution of the shielding effects may reveal a more pronounced difference in $\boldsymbol{U}_{\mathrm{eff}}/\boldsymbol{W}$.

Effect of oligomer elongation (2O•*X* to 3O•*X*)

To enhance the conductivities of the oligoEDOT-based conductors with consistently high $\boldsymbol{W}$ values (≈1 eV), decreasing the $\boldsymbol{U}_{\mathbf{eff}}$ is necessary. One method of decreasing $\boldsymbol{U}_{\mathbf{eff}}$ is to expand the π-conjugate areas of donors. Previous theoretical studies[15] predicted that extending the oligomer lengths in oligoacenes and oligothiophenes will result in a favorable decrease in $\boldsymbol{U}_{\mathrm{eff}}$. Thus, we focused on the strengths of oligomer conductors with extendable oligomer chain lengths, which systematically expanded the π-conjugate areas. The oligomer elongation effects on their conductivity were experimentally demonstrated in a quantitative manner for the first time by extending the donor from a dimer to a trimer (i.e., **2O** to **3O**) in a charge-transfer salt (Figure 1).[8]

We first synthesized the single-crystal salt, **3O**•$PF_6(CH_2Cl_2)_l$ via the electrooxidation of neutral **3O**. Like **2O**•PF_6, the molar ratio of donors and anions is 1:1, leading to a half-filled electronic structure (Figure 4a,b) . The calculated band structure showed a small gap around the

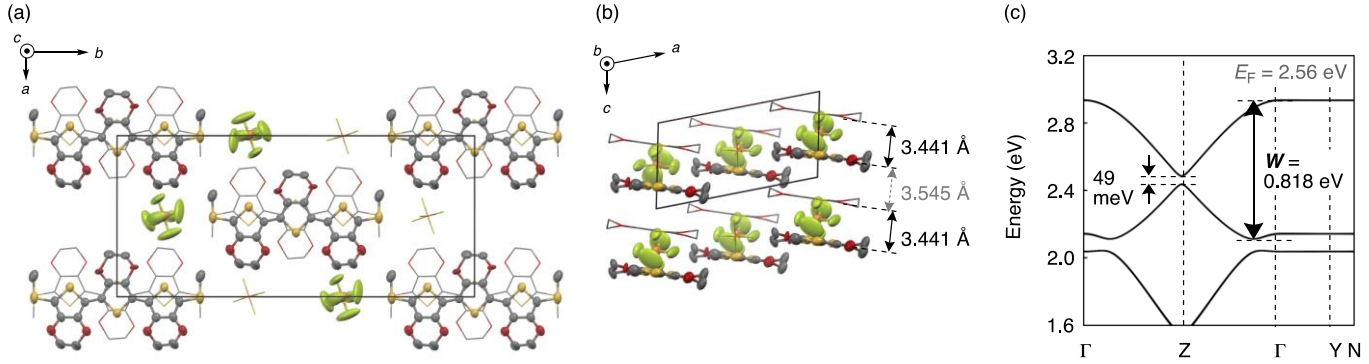

Figure 4. (a,b) Single-crystal structure of **3O**•$PF_6(CH_2Cl_2)_l$ along the (a) *c*-axis and (b) *b*-axis.[8] Atoms were colored as follows; red: oxygen; yellow: sulfur; gray: carbon; yellowish green: fluorine; orange: phosphorous. Hydrogens were omitted for clarity. (c) QE-calculated band structure of **3O**•PF_6 $PF_6(CH_2Cl_2)_l$. Γ (0,0,0), Z (0,0,0.5), Y (0,0.5,0), N (0,0.5,0.5).

Fermi level (Figure 4c), which can be classified as a band insulator. The ***W*** of **3O**•$PF_6(CH_2Cl_2)_I$, including the gap, was (0.818 eV),[10] which is slightly lower than that of **2O**•PF_6 (0.985 eV)[10] but still large among organic conductors.[3] The electrical conductivity of **3O**•$PF_6(CH_2Cl_2)_I$, was semiconducting, with approximately 2% of ρ_{rt} (1.0×10^3 Ω cm)[8] in relation to that of **2O**•PF_6. The E_a is 0.197 eV,[8] which is significantly smaller than that of **2O**•PF_6 (0.278 eV)[7] with an identical anion. Based on the E_a and calculated ***W***, the U_{eff}^{exp} (1.21 eV) and U_{eff}^{exp}/W (1.48) values were estimated to be 1.21 eV and 1.48, respectively,[10] which are smaller than those of **2O**•PF_6 (1.54 eV and 1.56, respectively).[10] These results confirm that extending the oligomer chain length efficiently improved the conductivity as theoretically predicted, even in the band-insulating state. Therefore, further extension of the oligomer chain length along the long and short molecular axes may further enhance the conductivity.

Effect of band-filling modulation (2O–HSO_4)

Band-filling modulation is another effective method of decreasing the U_{eff}. The previous oligoEDOT conductors are in half-filled states, which is rare for highly conductive molecular conductors. A subtle deviation in band filling of the half-filled materials which display the highest U_{eff} values can drastically reduce the U_{eff}. Hence, band-filling modulation was first investigated using **2O**–HSO_4, wherein a HSO_4^- anion under acid dissociation equilibrium conditions was used as the counter anion of **2O** (i.e., **2O**–HSO_4, Figure 1).[9] The crystal structure of **2O**–HSO_4 exhibits a 1:1 molar ratio of donors and anions, in which the anions form two types of disordered infinite one-dimensional chains (Figure 5a,b). Along the anion chains, the donors are uniformly π-stacked head-to-head, unlike the head-to-tail manner observed in **2O**•*X* and **3O**•$PF_6(CH_2Cl_2)_I$ (Figures 2a, 3a, and 4a). The π–π stacking distances of the donors are 3.441 Å (Figure 5b),[9] which is shorter than those of **2O**•*X* (3.46–3.48 Å).[7] The positions and number of protons could not be determined owing to their crystallographically specific positions. However, the O–O distances (2.33(3) and 2.98(3) Å) between the neighboring anion molecules (Figure 5b),[9] which are smaller than the sum of the van der Waals radii (3.04 Å), suggest the formation of proton-mediated hydrogen bonds in the chain, possibly enabling the partial removal or addition of protons.

Additional structural analysis for the bond-length alternation of the donors in the salt enabled us to estimate the valence of the donor. The weakening of the bond-length alternation of **2O**–HSO_4[9] upon oxidation by neutral **2O** is similar to those of half-filled **2O**•*X*,[7] indicating a valence of approximately +1. Assuming that the donor charge is +1, QE[11,12] was used for the first time to determine the band structure of **2O**–HSO_4 that does not induce a gap at the Fermi level (Figure 5c). The calculated ***W*** value was 0.943 e V, which is slightly lower than those of head-to-tail-type **2O**•*X* (0.979–1.01 eV) and may be attributed to the head-to-head stacking of the donors that weakened the orbital overlap. Further, the U_{eff}^{calc} of **2O**–HSO_4 was estimated using QE[11,12]/RESPACK[14] to be 2.31 eV, which is comparable to **2O**•*X* (2.33–2.43[10] eV). Due to its unfavorably reduced ***W*** (0.943 eV) in relation to those of **2O**•*X* (0.979–1.01 eV), its estimated U_{eff}^{calc}/W (2.45) is unfavorably higher than those of **2O**•*X* (2.34–2.46), predicting that **2O**–HSO_4 has a poorer conductivity than **2O**•*X*.

In contrast to the prediction, the electrical conductivity of **2O**–HSO_4 improved significantly, with a drastically lower ρ_{rt} of 3.1 Ω cm,[9] which is 0.007% of that of **2O**•PF_6 (4.3×10^4 Ω cm).[7] Although the semiconducting behavior was retained, it exhibited the smallest E_a (0.0886 eV)[9] among those of the oligoEDOT salts, and can thereby be regarded as a narrow-gap semiconductor. Considering the unfavorably small ***W***, the dramatic improvement in conductivity may be ascribed to the remarkably reduced U_{eff}, although the calculated U_{eff}/W for **2O**–HSO_4 (2.45) was unfavorably high or comparable to those of less conductive **2O**•*X* (2.34–2.46) under the assumption that the donor's valency is +1. Thus, we doubt the assumption. The addition or depletion of protons in the anion chains can alter the donor's valency from +1, although the valency appears to be approximately +1, which is apparent from the single-crystal bond-length analyses. The donor's valency not equal to +1 can deviate the band filling from the half-filled state, potentially reducing the U_{eff}. This hypothesis is experimentally demonstrated to be true by the considerably lower peak-top energy (0.65 eV) of the polarized reflectivity spectrum for single-crystal **2O**–HSO_4 than those for **2O**•*X* (0.72–0.74 eV).[9] Therefore, even a subtle change in the donor's valency from +1 can significantly impact the conductivity improvement, emphasizing the importance of band-filling modulation from the half-filled state that displays the maximum U_{eff}.

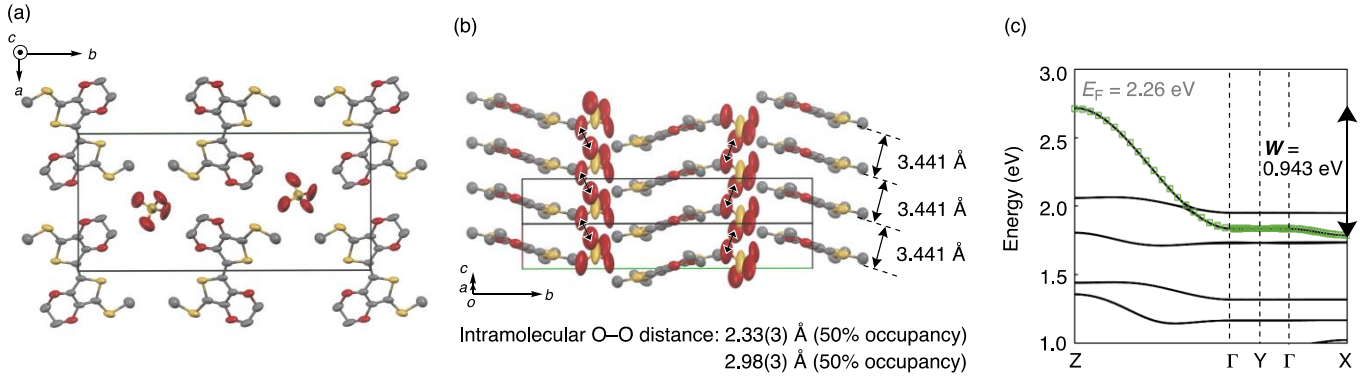

Figure 5. Single-crystal of **2O**–HSO_4 (a) along the *c*-axis and (b) from the perpendicular to the π-stacking direction. Atoms were colored as follows; red: oxygen; yellow: sulfur; gray: carbon. Hydrogens were omitted for clarity. (c) Band structure of **2O**–HSO_4. Z (0,0,0.5), Γ (0,0,0), Y (0,0.5,0), X (0.5,0,0).

Combined effect of oligomer elongation and band-filling modulation (4PS•$(PF_6)_{1.2}$(solvent)$_m$)

Finally, we combined the extending effect of the oligomer length and the band-filling modulation from the half-filled state. We designed an extended tetramer donor **4PS** comprising a **P**-**S**-**S**-**P** sequence, in which **S** is 3,4-ethylenedithiothiophene and **P** is 3,4-(2',2'-dimethylpropylenedioxy)thiophene (Figure 1).[10] The electrochemical oxidation of **4PS** yielded the single-crystal charge-transfer salt **4PS**•$(PF_6)_{1.2}$(solvent)$_m$.[10] The single-crystal structure exhibits pitched π-stacked donors (Figure 6a,b) with a quasi-1D (q1D) electronic structure, which was first observed in oligoEDOT systems. This may be attributed to the outer bulky **P** monomer units. Noticeably, the single-crystal structure displays unique columnar voids that contain additional solvent (acetone or H_2O) and 0.2 equivalents of PF_6^- anions, along with the equivalent PF_6^- anions relative to the donors (Figure 6b). This is apparent based on the results obtained via single-crystal XRD, energy-dispersive X-ray, and inductively coupled plasma atomic emission spectroscopy (ICP-AES).[10] The total 1.2 equivalents of anions caused the band filling to deviate from the half-filled state, and the extended length of conjugation significantly improved the conductivity.

Above room temperature, **4PS**•$(PF_6)_{1.2}$(solvent)$_m$ exhibited metallic behavior, with a low ρ_{rt} of 0.028 Ω cm (Figure 6c),[10] which is six-fold lower than that of **2O**•PF_6[7] with the identical counter anion. This metallic state was observed for the first time in the single-crystalline oligoEDOT system. The metallic state was further confirmed by observing the plasma reflection in the polarized reflectivity along the π-stacking direction, in addition to the magnetic characteristics.[10] In this metallic state, the E_a value is considered to be 0. As a result, the U_{eff}^{exp}/W ratio equals 1. The mixed sequence unique to the oligomer motif enables us to increase the oligomer length to expand the π-conjugate area, form a q1D electronic structure, and modulate the band filling. These combined effects dramatically improved the conductivity of the metallic state.

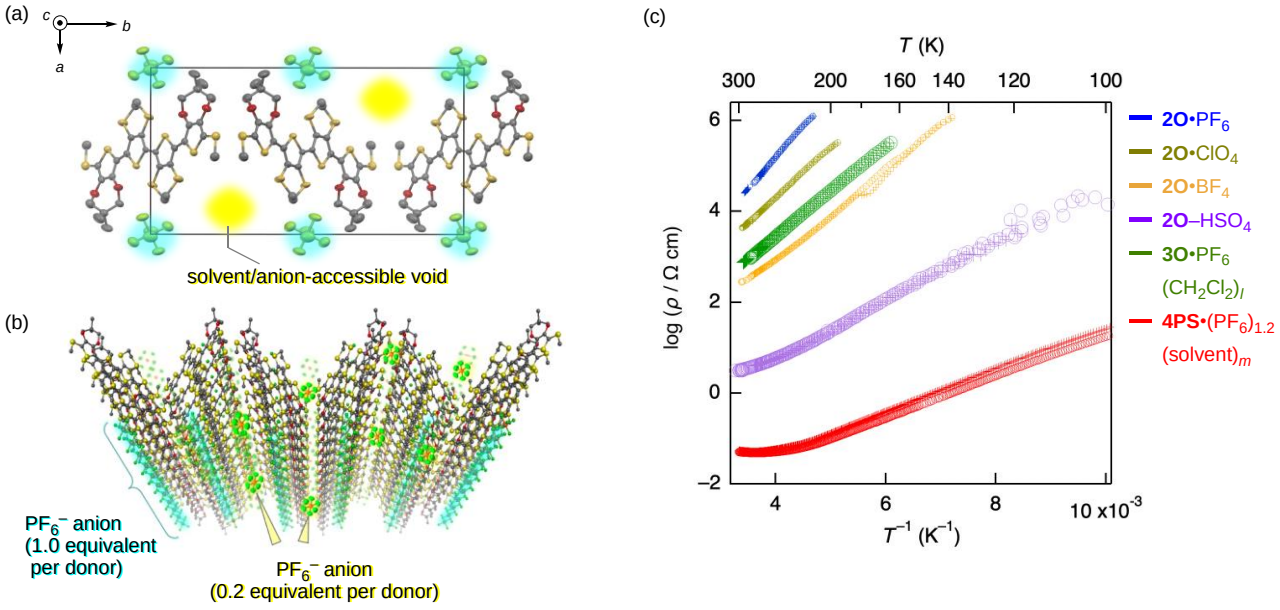

Figure 6. (a) Single-crystal structure of **4PS**•$(PF_6)_{1.2}$(solvent)$_m$ along the *c*-axis. (b) The packing structure of **4PS**•$(PF_6)_{1.2}$(solvent)$_m$ with 1.0 equivalent ordered PF_6^- anions (with aqua background) with illustrated 0.2 equivalents of disordered PF_6^- anions in the columnar voids. Atoms were colored as follows; red: oxygen; yellow: sulfur; gray: carbon; yellowish green: fluorine; orange: phosphorous. Hydrogens were omitted for clarity. (c) Electrical conductivity of oligoEDOT conductors.

The conductivity of single-crystal oligoEDOT-based conductors varied greatly, with ρ_{rt} values ranging from 10^{-2} to 10^6 Ω cm[7–10] depending on the donor structures and packing modes. We plotted ~~the values of~~ the experimentally determined ρ_{rt}, E_a, and U_{eff}^{exp},[7] and calculated U_{eff}^{calc}, W, and U_{eff}^{exp}/W, which were consistently evaluated by QE[11,12]/RESPACK for the first time,[14] to reference the distances between S atoms of the terminal methylthio groups (d_{SS}; Figure 7). These comprehensive analyses ~~plots~~ show that the tendencies of ρ_{rt} and E_a in reference to d_{SS} highly correlate to not only U_{eff}^{exp}/W but also U_{eff}^{exp} and U_{eff}^{calc}. These data emphasize the highly dominant contribution of U_{eff} in their conductivity, which may be characteristic of oligoEDOT-based conductors. The widely and systematically varied U_{eff} values, along with the W based on the packing structure of conductors, enabled the precise and flexible tuning of electronic structures by dual electronic parameters of U_{eff} and W. Based on this unique feature of oligoEDOT systems, a metallic state has been achieved with **4PS**•$(PF_6)_{1.2}$(solvent)$_m$ by dramatically reducing U_{eff}, reminiscent of the early stage of deviating from the strong electron correlations.

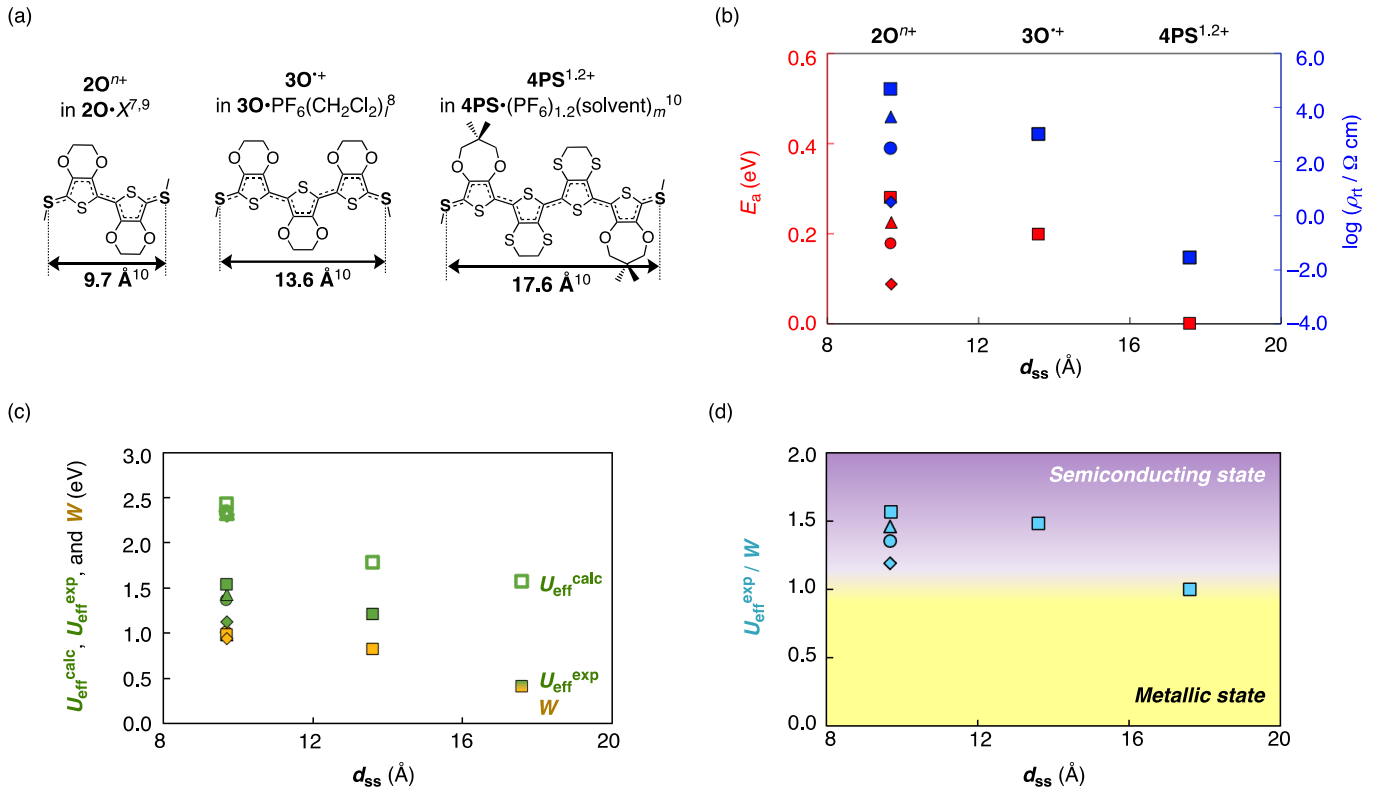

Figure 7. (a) S–S distance (d_{SS})[10] in the donor of single-crystal charge-transfer salts as the indicator of the conjugate length. (b,c,d) A summary of physical properties of oligomer-based conductors with a reference to d_{SS}. (b) E_a (red) and ρ_{rt} (blue) values. (c) U_{eff}^{calc}, U_{eff}^{exp}, and W values. (d) U_{eff}/W values. Data for PF_6^- (square), ClO_4^- (triangle), BF_4^- (circle), HSO_4^- (diamond) salts were plotted.

Conclusion

We constructed a library of oligoEDOT-based conductors[7–10] as single-crystal models for the doped PEDOT family.[2] Unlike conductive polymers with wide molecular weight distributions that render addressing the structural details and conductive mechanisms challenging, the use of single-crystal XRD of oligoEDOT conductors provided atomic-level structural data. We investigated the effects of the counter anion variation, oligomer length, and band-filling modulation from the half-filled state on conductivities. The consistent evaluations of the electronic structural insights for the screening study by theoretical calculations based on the single-crystal structural data addressing the correlation between the electronic structure and electric conductivity. These systematic investigations confirmed the unique electronic features of oligoEDOT systems with large W and widely variable U_{eff} values, which can enhance the conductivity of **4PS**•$(PF_6)_{1.2}$(solvent)$_m$ up to the metallic state above room temperature.[10] The single-crystal **2O**•X, **3O**•$PF_6(CH_2Cl_2)_I$, and **2O**–HSO_4 act as semiconductors in strongly correlated systems,[7–9] wherein U_{eff} dominated W because of the relatively short oligomer lengths. In contrast, the metallic **4PS**•$(PF_6)_{1.2}$(solvent)$_m$ above room temperature with a relatively elongated oligomer motif reduced U_{eff} to be equal to W, which is a sign of the deviation from the strong electron correlations. Further investigations may improve the conductivity using small anions, expanding the π-conjugate areas, and modulating band fillings.[15]. OligoEDOT-based conductors have high molecular designability and unique electronic states, which may offer a novel avenue in the field of molecular conductors towards weakly correlated systems.

Experimental

First-principles calculations for the electronic structures of **2O**•ClO_4, **2O**•BF_4, and **2O**–HSO_4 were performed based on the single-crystal structure data using the QE package[11,12] with the Generalized Gradient Approximation[16] as the exchange-correlation function, like preceding study on **2O**•PF_6, **3O**•$PF_6(CH_2Cl_2)_I$, and **4PS**•$(PF_6)_n$(solvent)$_m$.[10] In the calculations, SG15 Optimized Norm-Conserving Vanderbilt (ONCV) pseudopotentials[17] were used as the pseudopotentials. The cutoff kinetic energies for the wave functions, charge densities, and mesh of the wave numbers were set as 80, 320 Ry, and 3 × 3 × 5 and 5 × 3 × 3 (**2O**•BF_4 and **2O**•ClO_4, respectively. After the self-consistent field (scf) calculation, non-scf calculation was performed. Using these data, maximally localized Wannier functions (MLWFs) were obtained using RESPACK,[14] and the bands near the Fermi energy were selected to reproduce the MLWFs, providing the Wannier interpolation bands near the Fermi energy obtained by QE[11,12] and the Wannier interpolation. Using H-wave (https://isspns-gitlab.issp.u-tokyo.ac.jp/hwave-

dev/hwave-gallery//tree/main/samples/ UHFk/dos_plot), a mean-field approximation program, based on the MLWFs, the density of states (DOS) was calculated for the quantification of $\boldsymbol{W}$. The $\boldsymbol{U}_{\mathbf{eff}}^{\mathbf{calc}}$ values were calculated by RESPACK,[14] in which the Coulomb interaction is reduced owing to screening effects from bands other than the target band. Using a constrained random phase approximation (cRPA) method, we can obtain the screened Coulomb interactions $\boldsymbol{U}_{\mathbf{eff}}$ by incorporating screening effects from non-target bands. Through previous reports of such applications to different organic material systems,[18–20] we know that the effective Hamiltonian models derived by the cRPA method can successfully evaluate the stability of competing phases in electron-correlated systems. Thus, we estimated the Coulomb interactions by using the cRPA method. The energy cutoff for the dielectric function was set to 5.0 Ry. Static screened direct integrals were calculated as the matrix element of the shielded Coulomb interaction between the Wannier functions. The values at 0 Å were used as the $\boldsymbol{U}_{\mathbf{eff}}^{\mathbf{calc}}$.

Conflicts of interest

There are no conflicts of interest to declare.

Acknowledgements

The authors would like to thank Idemitsu Kosan Co., Ltd. for their support throughout this study. This work was partially supported by JSPS Grants-in-Aid for Scientific Research (No. JP16H04010, JP17K18746, JP18H05225, JP21K18597, JP22H00106 to H.M., JP20H05206, JP21K05018, JP22H04523 to T.F., JP20K15240 to S.D.), JSPS Research Fellowships for Young Scientists and University Fellowship to JP23KJ0577 to K.O.), JST PRESTO (JPMJPR22Q8 to T.F.), JST Founding Project for Innovation Creation in Science and Technology (The Univ. of Tokyo) to K.O. MEXT Grants-in-Aid for Scientific Research on Innovative Areas “Hydrogenomics” (JP18H05516 to H.M.), a research grant from the Iketani Sci. and Technol. Foundation, the Naito Foundation, the Kao Foundation for Arts and Science to T.F., a research grant from the Noguchi Institute to S.D. The authors would also like to thank the Supercomputer Center, The Institute for Solid State Physics, and The Univ. of Tokyo for the use of their facilities.

Notes and references

1 Facchetti, A. π-Conjugated Polymers for Organic Electronics and Photovoltaic Cell Applications. *Chem. Mater.* **2011**, *23*, 733–758.
2 Elschner, A.; Kirchmeyer, S.; Lövenich, W.; Merker, U.; Reuter, K. PEDOT: Principles and Applications of an Intrinsically Conductive Polymer, 1st. ed.; CRC Press, **2010**. 164–264 and 293–328.
3 Kagoshima, S.; Nagasawa, H.; Sambongi, T. One-Dimensional Conductors; Springer-Verlag, BerlinHeidelberg **1988**, 48–105.
4 Imada, M.; Fujimori, A.; Tokura, Y. Metal-insulator Transitions. *Rev. Mod. Phys.* **1998**, *70*, 1039–1263.
5 Müllen, K.; Wegner, G. *Electronic Materials: The Oligomer Approach*, Wiley—VCH Verlag GmbH, Weinheim, **1998**.
6 Tahara, T.; Suzuki, S.; Kozaki, M.; Nishinaga, T.; Okada, K. Chemical Stability of the 5-Mesityl-5′′-(nitronyl nitroxide)-2,2′:5′,2′′-ter(3,4-ethylenedioxythiophene) Radical Cation. *Bull. Chem. Soc. Jpn.* **2018**, *91*, 1193–1195.
7 Kameyama, R.; Fujino, T.; Dekura, S.; Kawamura, M.; Ozaki, T.; Mori, H. The Simplest Model for Doped Poly(3,4-ethylenedioxythiophene) (PEDOT): Single-crystalline EDOT Dimer Radical Cation Salts. *Chem. Eur. J.* **2021**, *27*, 6696–6700.
8 Kameyama, R.; Fujino, T.; Dekura, S.; Mori, H. Conjugation Length Effect on the Conducting Behavior of Single-Crystalline Oligo(3,4-ethylenedioxythiophene) (*n*EDOT) Radical Cation Salts. *Phys. Chem. Chem. Phys.* **2022**, *24*, 9130–9134.
9 Kameyama, R.; Fujino, T.; Dekura, S.; Imajo, S.; Miyamoto, T.; Okamoto, H.; Mori, H. Band-Filling Effects in Single-Crystalline Oligomer Models for Doped PEDOT: 3,4-Ethylenedioxythiophene (EDOT) Dimer Salt with Hydrogen-Bonded Infinite Sulfate Anion Chains. *J. Mater. Chem. C* **2022**, *10*, 7543–7551.
10 Onozuka, K.; Fujino, T.; Kameyama, R.; Dekura, S.; Yoshimi, K.; Nakamura, T.; Miyamoto, T.; Yamakawa, T.; Okamoto, H.; Mori, H. Metallic State of a Mixed-sequence Oligomer Salt That Models Doped PEDOT Family. *J. Am. Chem. Soc.* **in press**. DOI: 10.1021/jacs.3c01522.
11 Giannozzi, P.; Baroni, S.; Bonini, N.; Calandra, M.; Car, R.; Cavazzoni, C.; Ceresoli, D.; Chiarotti, G. L.; Cococcioni, M.; Dabo, I.; Dal Corso, A.; de Gironcoli, S.; Fabris, S.; Fratesi, G.; Gebauer, R.; Gerstmann, U.; Gougoussis, C.; Kokalj, A.; Lazzeri, M.; Martin-Samos, L.; Marzari, N.; Mauri, F.; Mazzarello, R.; Paolini, S.; Pasquarello, A.; Paulatto, L.; Sbraccia, C.; Scandolo, S.; Sclauzero, G.; Seitsonen, A. P.; Smogunov, A.; Umari, P.; Wentzcovitch, R. M. QUANTUM ESPRESSO: A Modular and Open-Source Software Project for Quantum Simulations of Materials. *J. Phys. Condens. Matter* **2009**, *21*, 395502.
12 Giannozzi, P.; Andreussi, O.; Brumme, T.; Bunau, O.; Buongiorno Nardelli, M.; Calandra, M.; Car, R.; Cavazzoni, C.; Ceresoli, D.; Cococcioni, M.; Colonna, N.; Carnimeo, I.; Dal Corso, A.; de Gironcoli, S.; Delugas, P.; DiStasio, R. A.; Ferretti, A.; Floris, A.; Fratesi, G.; Fugallo, G.; Gebauer, R.; Gerstmann, U.; Giustino, F.; Gorni, T.; Jia, J.; Kawamura, M.; Ko, H. Y.; Kokalj, A.; Küçükbenli, E.; Lazzeri, M.; Marsili, M.; Marzari, N.; Mauri, F.; Nguyen, N. L.; Nguyen, H. V.; Otero-de-la-Roza, A.; Paulatto, L.; Poncé, S.; Rocca, D.; Sabatini, R.; Santra, B.; Schlipf, M.; Seitsonen, A. P.; Smogunov, A.; Timrov, I.; Thonhauser, T.; Umari, P.; Vast, N.; Wu, X.; Baroni, S. Advanced Capabilities for Materials Modelling with QUANTUM ESPRESSO. *J. Phys. Condens. Matter* **2017**, *29*, 465901.
13 Momma, K.; Izumi, F. *VESTA*: A Three-dimensional Visualization System for Electronic and Structural Analysis. *J. Appl. Crystallogr.* **2008,** *41*, 653–658.
14 Nakamura, K.; Yoshimoto, Y.; Nomura, Y.; Tadano, T.; Kawamura, M.; Kosugi, T.; Yoshimi, K.; Misawa, T.; Motoyama, Y. RESPACK: An Ab Initio Tool for Derivation of Effective Low-Energy Model of Material. *Comput. Phys. Commun.* **2021**, *261*, 107781.
15 Mori, H.; Kamiya, M.; Haemori, M.; Suzuki, H.; Tanaka, S.; Nishio, Y.; Kajita, K.; Moriyama, H. First Systematic Band-Filling Control in Organic Conductors. *J. Am. Chem. Soc.* **2002**, *124*, 1251–1260.
16 Perdew, J. P.; Burke, K.; Ernzerhof, M. Generalized Gradient Approximation Made Simple. *Phys. Rev. Lett.* **1996**, *77*, 3865–3868.
17 Schlipf, M.; Gygi, F. Optimization Algorithm for the Generation of ONCV Pseudopotentials. *Comput. Phys. Commun.* **2015**, *196*, 36–44.

18 Ido, K.; Yoshimi, K.; Misawa, T.; Imada, M. Unconventional Dual 1D–2D Quantum Spin Liquid Revealed by Ab Initio Studies on Organic Solids Family. *npj Quantum Mater.* **2022**, *7*, 1–10.
19 Ohki, D.; Yoshimi, K.; Kobayashi, A.; Misawa, T. Gap Opening Mechanism for Correlated Dirac Electrons in Organic Compounds α-(BEDT-TTF)$_2$I$_3$ and α-(BEDT-TSeF)$_2$I$_3$. *Phys. Rev. B* **2023**, *107*, L041108.
20 Yoshimi, K.; Misawa, T.; Tsumuraya, T.; Seo, H. Comprehensive *Ab Initio* Investigation of the Phase Diagram of Quasi-One-Dimensional Molecular Solids. *Phys. Rev. Lett.* **2023**, *131*, 036401.